Published in final edited form as:
J Nucl Med. 2013 March ; 54(3): 373–379. doi:10.2967/jnumed.112.110601.

Myocardial Perfusion Imaging with a Solid State Camera: Simulation of a Very Low Dose Imaging Protocol

Ryo Nakazato[1], **Daniel S. Berman**[1], **Sean W. Hayes**[1], **Mathews Fish**[2], **Richard Padgett**[3], **Yuan Xu**[1], **Mark Lemley**[2], **Rafael Baavour**[4], **Nathaniel Roth**[4], and **Piotr J. Slomka**[1]

[1]Cedars-Sinai Medical Center, Cedars-Sinai Heart Institute, Los Angeles, CA, USA

[2]Oregon Heart & Vascular Institute, Sacred Heart Medical Center, Springfield, OR, USA

[3]Oregon Heart & Vascular Institute, Sacred Heart Medical Center, Oregon Cardiology, Springfield, OR, USA

[4]Spectrum Dynamics, Caesarea, Israel

Abstract

High sensitivity dedicated cardiac systems cameras provide an opportunity to lower injected doses for SPECT myocardial perfusion imaging (MPI), but the exact limits for lowering doses have not been determined. List mode data acquisition allows for reconstruction of various fractions of acquired counts, allowing a simulation of gradually lower administered dose. We aimed to determine the feasibility of very low dose MPI by exploring the minimal count level in the myocardium for accurate MPI.

Methods—Seventy nine patients were studied (mean body mass index 30.0 ± 6.6, range 20.2–54.0 kg/m^2) who underwent 1-day standard dose ^{99m}Tc-sestamibi exercise or adenosine rest/stress MPI for clinical indications employing a Cadmium Zinc Telluride dedicated cardiac camera. Imaging time was 14-min with 803 ± 200 MBq (21.7 ± 5.4mCi) of ^{99m}Tc injected at stress. To simulate clinical scans with lower dose at that imaging time, we reframed the list-mode raw data to have count fractions of the original scan. Accordingly, 6 stress equivalent datasets were reconstructed corresponding to each fraction of the original scan. Automated QPS/QGS software was used to quantify total perfusion deficit (TPD) and ejection fraction (EF) for all 553 datasets. Minimal acceptable count was determined based on previous report with repeatability of same-day same-injection Anger camera studies. Pearson correlation coefficients and SD of differences with TPD for all scans were calculated.

Results—The correlations of quantitative perfusion and function analysis were excellent for both global and regional analysis on all simulated low-counts scans (all $r \geq 0.95$, $p < 0.0001$). Minimal acceptable count was determined to be 1.0 million counts for the left ventricular region. At this count level, SD of differences was 1.7% for TPD and 4.2% for EF. This count level would correspond to a 92.5 MBq (2.5 mCi) injected dose for the 14 min acquisition.

Conclusion—1.0 million myocardial count images appear to be sufficient to maintain excellent agreement quantitative perfusion and function parameters as compared to those determined from 8.0 million count images. With a dedicated cardiac camera, these images could be obtained over

Address for Correspondence: Piotr Slomka, PhD, Department of Imaging, Cedars-Sinai Medical Center, 8700 Beverly Boulevard, Taper Building Suite A047, Los Angeles, CA 90048, USA, Phone: 310-423-4348, Fax: 310-423-0171, slomkap@cshs.org.
First author: Ryo Nakazato, MD, PhD, Department of Imaging, Cedars-Sinai Medical Center, 8700 Beverly Boulevard, Taper Building Suite 1258, Los Angeles, CA 90048, USA, Phone: 310-994-1940, Fax: 310-423-8396, Ryo.Nakazaro@cshs.org

Conflicts of interest:
Dr. Daniel Berman is a shareholder in Spectrum-Dynamics. Rafael Baavour and Nathaniel Roth are Spectrum-Dynamics company employees. All others disclose no conflict of interest.

10 minutes with an effective radiation dose of less than 1 mSv without significant sacrifice in accuracy.

Keywords

myocardial perfusion imaging; counts; cadmium-zinc-telluride; simulation study; quantification

Reducing patient radiation exposure has become an important challenge for nuclear cardiology. The last few years have brought several rapid developments in nuclear cardiology instrumentation in scanner hardware increasing photon sensitivity. Additionally, new SPECT reconstruction software methods on conventional and dedicated systems have preserved or improved SPECT image quality even with lower count statistics (1–9). As a result acquisition time for SPECT myocardial perfusion imaging (MPI) may be significantly shortened. Several new dedicated camera systems with optimized acquisition geometry and collimator design resulting in increased count sensitivity have been introduced by vendors (10–16). While it is convenient for patients to have imaging completed in 2–4 minutes, the efficiency of these systems provides the opportunity to reduce both the time of acquisition and the radiation dose to the patient. The degree to which the radiation dose can be reduced, while simultaneously reducing scan acquisition times, has not been explored.

List mode data acquisition available in new systems allows for reconstruction of various fractions of acquired counts, so that a simulation of various levels of lower administered dose can be performed. We aimed to determine the minimal count level in the left ventricular region for the dedicated cardiac system with cadmium-zinc-telluride (CZT) detectors that could provide accuracy similar to standard Anger camera. We focused on stress MPI data to simulate the minimal number of counts in a stress scan, with application to very low dose stress-only protocols (17).

MATERIALS AND METHODS

Study Patients

We evaluated 79 consecutive patients who underwent MPI using a CZT camera (D-SPECT, Spectrum-Dynamics, Caesarea, Israel). Patients were referred for evaluation by rest-stress MPI for clinical indications. Prior to scanning, we collected information on the presence of categorical cardiac risk factors in each individual. Hypertension was defined on the basis of a documented history of hypertension and/or treatment with anti-hypertensive medications. Diabetes mellitus was defined based on a clinical history of diabetes and/or use of insulin or oral hypoglycemic agents. Dyslipidemia was also defined based on clinical history and/or use of lipid-lowering medications. A positive smoking history was defined as current smoking or smoking cessation less than 3 months prior to MPI testing. Family history of coronary artery disease was defined as myocardial infarction or cardiac death before age 55 in a man and before age 65 in a woman as reported by patient query. The occurrence of a prior myocardial infarction was based on either an initial report by the patient or chart documentation. This study was conducted according to guidelines of the Oregon Heart & Vascular Institute Institutional Review Board. All patients provided written informed consent for the use of their clinical and imaging data for research purposes.

Patient Preparation and Image Acquisition

Patients were instructed to abstain from any products containing caffeine for 24 h before the test. Beta-blockers and calcium-channel antagonists were discontinued for 48 hours, and nitrates for 6 hours, before testing. Rest/stress 1-day ^{99m}Tc-sestamibi imaging was performed in all patients using weight-adjusted doses of 111–296 MBq (3–8 mCi) for rest

and 481–1221 MBq (13–33 mCi) for stress (12), in the upright position. Rest images were not used in this study as we focused on simulations which could be applicable to stress-only protocols (17–19). Patients underwent symptom-limited standard exercise treadmill testing (51%) or adenosine stress (49%, 140 μg/kg/min for 6 minutes) with injection at peak stress (20,21). Stress imaging was begun at 15 to 30 min after injection and followed by a 14-min acquisition. With regard to the administered dose of ^{99m}Tc-sestamibi to the patients, we have found that an average of 74 MBq (2 mCi) remains in the syringe and the injection tubing (unpublished data).

A full description of the dedicated cardiac system used here has been previously reported (13,22,23). Briefly, the system uses 9 tungsten collimated CZT detector columns rotating in synchrony, each consisting of 1024 (16 × 64), 5-mm thick CZT elements (2.46 × 2.46 mm). The size of the collimator holes matches the dimensions of the detector elements. Before imaging, the detector was positioned parallel to the patient's chest, with the heart in the center of the field of view. A 6 to 12-sec pre-scan acquisition was performed to identify the location of the heart and to set the angle limits of scanning for each detector column (region-of-interest centric scanning). Each image set was acquired with 120 projections per detector.

The vendor reconstruction includes 2 steps. A first reconstruction step uses a uniform grey starting image with 3 iterations. In this step the left ventricular (LV) region is determined for the LV counts calculation. This approximate LV region reconstruction is subsequently used as a prior for the further reconstruction of the full image data with additional 4 iterations. This final transaxial image is generated from list mode data by the vendor reconstruction algorithm based on the maximum likelihood expectation maximization method (23) with resolution recovery using a total of 4–7 iterations and 32 subsets and an additional inter-iterative kernel convolution smoothing (12). These parameters are the default reconstruction parameters validated in the previous study (12), where image quality and quantitative parameters were compared to the conventional MPI. No attenuation or scatter correction was applied. Images were then automatically reoriented into short-axis and vertical and horizontal long-axis slices using standard software (QPS, Cedars-Sinai Medical Center, Los Angeles, California).

Left Ventricular Count Determination

The LV counts were determined from the planar projections of the approximate LV region defined during the first step of data reconstruction. We could not use the reconstructed image data and accurate 3D LV segmentation, since the vendor adjusts the reconstructed counts to account for the efficiency of the detectors and collimators. During this first reconstruction step, a circular ROI is adjusted by the observer around the LV on the transaxial, coronal and sagital projections. Subsequently the volumetric ROI is back-projected on all of the detectors creating planar ROIs, which are used for the LV counts calculation. In this way, most of the extra-cardiac and background activity is eliminated.

Simulation of Lower Injected Dose

To simulate a clinical scan with lower counts acquired over the full acquisition time, the patient's list-mode raw data was reframed such that only a fraction of each view was used and subsequently these truncated views were reconstructed in the same manner as full count scans. For example, a 14-min scan 120-view scan acquired with 7 sec per view was reframed to a subset of the data with 3.5 sec per view to simulate half-dose images (Figure 1). Using this methodology, 6 low-count stress scans were reconstructed from each full-count reconstruction scan, to simulate various levels of myocardial counts [3.6 million counts (MC), 2.0 MC, 1.3 MC, 1.0 MC, 0.7 MC, 0.5MC]. The acquisition and reconstruction parameters were the same for all data used in the current study.

Image Analysis

Automated QPS/QGS software was used to quantify myocardial perfusion and function for all 553 datasets (7×79) (24). The quantitative perfusion variable employed was total perfusion deficit (TPD), which reflects a combination of both defect severity and the extent of the defect in one parameter, as previously described (25,26). On per-patient basis, abnormal stress TPD was defined as ≥5% and categorized as mild (5–10%) and moderate/severe (>10%) (27). Regional TPD was also calculated for each vascular territory, and ≥2% was defined as abnormal (26). We have analyzed these cases separately to assess the minimal counts required in abnormal patients.

From this population, we have generated a count-specific normal database using 34 patients (14 male, 20 female) who had a low likelihood of coronary artery disease (<10%) based on age, sex, symptoms, coronary risk factor and results of treadmill stress test at the time of MPI or who had normal rest and stress images by visual assessment (26). Stress perfusion defects were assessed by quantification of the TPD using these count-specific normal limits as well as standard limits previously obtained for this system (26). Left ventricular ejection fraction (EF) was quantified using a modified version of QGS (28) accounting for higher resolution and better visibility of the myocardial base (29).

Statistical Analysis

Continuous variables are presented as means ± SD and categorical variables as frequencies. Pearson's correlation coefficient, Bland-Altman limits of agreement and standard deviation (SD) of differences were calculated using original high-count study of 8.0 MC as the reference standard. A two-tailed $p < 0.05$ was considered statistically significant. Minimal acceptable count was determined based on a previous report with repeatability of same-day same-injection Anger camera studies (30). All statistical calculations were performed using STATA (Version 11, StataCorp LP, College Station, Texas, USA) for Windows.

RESULTS

The patient characteristics of the study population are given in Table 1. Mean body mass index (BMI) was 30.0 ± 6.6 kg/m^2 and ranged from 20.2 to 54.0 kg/m^2. Thirty-two out of 79 patients had abnormal stress TPD (≥5%) including 12 patients with mild stress perfusion defects (TPD 5–10%), 20 patients with moderate/severe stress perfusion defects (TPD >10%). In 32 patients with abnormal stress TPD, 8 had fixed perfusion defects, and 24 had reversible perfusion defects in the original 8.0 MC scans. Per vessel analysis, stress perfusion abnormality (TPD ≥2% per each vascular territory) was seen in 22, 22 and 19 patients in LAD, LCX and RCA territories, respectively. A mean dose of 802.9 ± 199.8 MBq (21.7 ± 5.4 mCi) of ^{99m}Tc-sestamibi for stress was drawn up in the syringe; assuming 74 MBq (2 mCi) to remain in the syringe and the injection tubing, 728.9 MBq (19.7 mCi) was administered to the patients. The average LV counts for stress scan were 7962719 ± 2349989, 3598744 ± 14929, 2000125 ± 7092, 1300958 ± 8121, 1000180± 5177 and 700363 ± 5332, 500760 ± 3964 for original, 3.6 MC, 2.0 MC, 1.3 MC, 1.0 MC, 0.7 MC and 0.5 MC, respectively.

Fourteen out of 553 myocardial contours generated from QPS needed adjustment for static perfusion images, as determined by an experienced imaging technologist without knowledge of quantitative results, with no relationship to the number of myocardial counts in the study (Table 2).

The reproducibility of simulated global perfusion and function results is shown in Table 3. The correlations of quantitative perfusion analysis were excellent for global analysis on all simulated low-count scans (all $r \geq 0.99$, $p < 0.0001$). At the level of 1.0 MC, SD of the

differences for TPD was 1.7%, and SD of the differences for EF was 4.2%. Bland–Altman analyses for global perfusion quantification are shown in Figure 2. Compared to the high-count (8.0 MC) reference standard, the reduced count studies showed a small negative bias, which increased in relationship to the number of MC; however, the Bland-Altman plots demonstrated that bias remained low through the range of simulated low-counts scans. In patients with abnormal stress perfusion defects (separately evaluated), the correlation was also excellent ($r = 0.99$, $p < 0.0001$) and SD of differences was 1.7% at the level of 1.0 MC. In patients without abnormal stress perfusion defects, the SD of differences was 1.2% at the level of 1.0 MC. The results were similar between patients with and without abnormal stress perfusion defects. In large patients with BMI >30 kg/m^2 ($n = 34$), the correlation was excellent ($r = 0.99$, $p < 0.0001$) and SD of differences was 1.4% at the level of 1.0 MC.

Figure 3 shows the bias of TPD values using the count-specific normal database compared to using the same normal database for different level of counts. The use of the count-specific database was associated with a significant reduction of TPD bias from 1.4% to 0.6% in the overall population. Similarly, in large patients with BMI >30 kg/m^2, TPD bias was on the average 22% lower with using count-specific normal database.

The reproducibility of simulated perfusion results for regional perfusion analysis is shown in Table 4. Correlation values were similar to those observed for global perfusion analysis on the simulated low-counts scans (all $r \geq 0.95$, $p < 0.0001$).

In a previous report with repeatability of same-day same-injection full count Anger camera studies, SD of the differences was 1.7% for TPD and 3.6% for EF (30). In the present study on 1.0 MC scan, SD was 1.7% for TPD and 4.2% for EF. There was no significant difference in SD for EF between these 2 studies ($p = 0.4$). Therefore, minimal acceptable count was determined to be 1.0 MC for stress CZT-MPI. For the 14 min acquisition, the 1.0 MC scan allows the injected dose to be reduced by a factor of 8, which corresponds to the average dose of 92.5 ± 25.9 MBq (2.5 ± 0.7 mCi) [range 51.8 to 144.3 MBq (1.4 to 3.9 mCi)] injected dose, and in this study would have resulted in the effective average radiation dose of 0.71 ± 0.20 mSv (range 0.40 to 1.11 mSv) in a 14 min study and the average radiation dose 0.99 ± 0.28 mSv (range 0.56 to 1.55 mSv) in a 10 min study. In large patients with BMI >30 kg/m^2 at the level of 1.0 MC (average counts 1001319), the average injected dose would be 111.0 ± 25.9 MBq (3.0 ± 0.7 mCi) [range 66.6 to 144.3 MBq (1.8 to 3.9 mCi)] with the average radiation dose of 0.85 ± 0.20 mSv (range 0.51 to 1.11 mSv) in a 14 min study.

Case examples of images at gradually reduced dose levels are shown in Figure 4 and 5.

DISCUSSION

Reducing effective radiation dose to patients and exposure nuclear staff is an important goal in the field of nuclear cardiology (31). Our study demonstrates that dedicated cardiac scanners may allow an acquisition with average LV region counts as low as 1.0 MC for stress MPI regardless of the presence of stress perfusion defects, while maintaining excellent agreement in quantitative perfusion and function parameters as compared to those determined from very high count images. We used the average doses administered in our calculations, and the estimate specific to a given patient may vary depending on the injected dose (based on patient's BMI). Therefore, the minimal dose could be higher in patients with higher BMI and lower in patients with lower BMI. For patients with BMI >30 kg/m^2 the average estimated radiation dose of 0.85 ± 0.20 mSv (range 0.51 to 1.11 mSv) at the 1 million count level was higher than in the overall study population (0.71 ± 0.20 mSv (range 0.40 to 1.11 mSv).

The findings show that the amount of injected radioactivity can be reduced by a factor of 8 with a 14-min acquisition, resulting in a 1.0 MC scan with a 92.5 MBq (2.5 mCi) injected dose, which would be associated with an average 0.71 mSv effective radiation dose to the patient (32). Since it is desirable to reduce both radiation dose and scan acquisition time, these findings further imply that by increasing the injected dose to 125.8 MBq (3.4 mCi), a "sub-mSv" stress-only MPI study can be achieved with an acquisition time of 10 min. However, a larger, prospective, multicenter trial warrants further investigation.

We established minimum count levels precisely by retrospective analysis of full-dose full-time data and reconstruction of only a fraction of the counts spread over full acquisition time. Such an approach is facilitated by the list-mode capabilities of the new scanners. Especially for the new stationary scanners, it is possible to retrospectively simulate a scan with an arbitrary activity or alternatively duration, from the original full-dose/full-time acquisition data. Using a similar approach, Herzog et al. have shown by the retrospective list-mode reconstruction that 2 min acquisition time is the most optimal for the GE Healthcare UFC scanner (14). In our study the data was acquired over full imaging time, and therefore the simulation should closely correspond to low-dose full time acquisition protocols.

The reference standard of 8.0 MC has very high count levels, which are much higher than currently obtained by Anger cameras. The reason why significant count reductions do not translate into poorer reproducibility is the high sensitivity of collimators used and the detector geometry focused on the cardiac region, rather than the use of the solid state detectors. This allows obtaining 6–8 times the count rate as compared to the conventional system. The acquisitions obtained with these new systems at standard doses and standard count rates have a very high count rate; therefore, significant reductions can be obtained still maintaining adequate image statistics. Similar simulation studies could be performed for other dedicated cardiac systems without solid detectors (4) or for new reconstruction methods (7,9) if list mode acquisition is available. Our findings show that there is little benefit in imaging with such high count levels as compared to low-count studies.

In the present study, we employed fully automated quantitative analysis of MPI studies. Quantitative analysis eliminates observer variability and bias, is useful for comparing sequential MPI studies (33,34). It also provides an approach that is more generalizable to other centers, as it is not dependent on the expertise of the interpreter. It should be mentioned that the reported variability is the overall variability due to the count level differences but also due to the intrinsic variability of the quantitative software (sampling methods, valve plane determination). However, this overall variability is the practical clinical measure by which the low dose imaging could be judged. We have demonstrated here that this overall variability for studies with gradually decreasing count levels (up to 8 times) is similar to the quantitative variability of the repeated studies with the same count levels obtained Anger camera.

It is noteworthy that the use of the same normal database for all count levels (26) was associated with increasing bias of TPD values. Count-specific databases allowed significant reduction of this bias. Therefore, our findings indicate that count-specific normal databases are needed to provide comparable findings for studies with different count levels, since the normal thresholds for perfusion studies could be affected by the bias.

The method used for the count estimation may overestimate the myocardial counts due to the approximate shape of the LV region. Although the use of 3D QGS/QPS boundaries could improve the results by excluding the background activity more precisely, in the current implementation of the vendor reconstruction, the tomographic counts could not be

used because they are scaled in order to correct for known detector and collimator efficiencies. However, the advantage of our method for the LV count estimation is that it is easily available to the scanner operator – without the need for additional software processing during image acquisition. Even if 3D LV counts have been estimated from the precise LV segmentation, the myocardial count levels would still be affected by the extent of the hypoperfusion. We have, however, shown good reproducibility in abnormal studies with a low count levels as well.

Our study has several limitations. The acquisitions were performed at only single center with one type of system; however, our application of automated quantitative analysis in this study increases the likelihood that our results could be replicated elsewhere. More importantly, due to the specialized high-dose full-time protocol which was employed only in a limited number of patients, we could not use a separate population for development of count-specific normal databases. However, we obtained the results separately in an abnormal population, and these results agree with the findings in the overall population. We included patients with a BMI ranging from 20.2 to 54.0 kg/m^2. However, mean BMI was 30.0 kg/m^2 in our population, therefore, caution must be taken when extrapolating average estimated dose to patients with a substantially higher body mass index. Therefore, we also provided ranges of the estimated doses and separately evaluated the doses for the patients with high BMI. We did not use attenuation correction since this camera is not equipped with that option.

CONCLUSION

This simulation study based on reframing of patient image data suggests that a dedicated cardiac scanner may allow counts as low as 1.0 MC for stress myocardial perfusion imaging, while maintaining excellent agreement in quantitative perfusion and function parameters as compared to those determined from high-count full-time images. Our findings suggest that a 10 min stress scan can be performed with an effective average radiation dose of less than 1 mSv with the dedicated cardiac scanners.

Acknowledgments

This research was supported in part by grant R01-HL089765 from the National Heart, Lung, and Blood Institute/ National Institutes of Health (NHLBI/NIH) (PI: Piotr Slomka). Its contents are solely the responsibility of the authors and do not necessarily represent the official views of the NHLBI. We would like to thank Arpine Oganyan for editing and proofreading the text.

References

1. DePuey EG, Gadiraju R, Clark J, Thompson L, Anstett F, Shwartz SC. Ordered subset expectation maximization and wide beam reconstruction “half-time” gated myocardial perfusion SPECT functional imaging: a comparison to “full-time” filtered backprojection. J Nucl Cardiol. 2008; 15:547–63. [PubMed: 18674723]
2. Borges-Neto S, Pagnanelli RA, Shaw LK, et al. Clinical results of a novel wide beam reconstruction method for shortening scan time of Tc-99m cardiac SPECT perfusion studies. J Nucl Cardiol. 2007; 14:555–65. [PubMed: 17679065]
3. Vija H, Chapman J, Ray M. IQ SPECT technology White Paper. Siemens Medical Solutions USA Molecular Imaging. 2008:1–7.
4. Venero CV, Heller GV, Bateman TM, et al. A multicenter evaluation of a new postprocessing method with depth-dependent collimator resolution applied to full-time and half-time acquisitions without and with simultaneously acquired attenuation correction. J Nucl Cardiol. 2009; 16:714–25. [PubMed: 19582531]

5. Maddahi J, Mendez R, Mahmarian JJ, et al. Prospective multicenter evaluation of rapid, gated SPECT myocardial perfusion upright imaging. J Nucl Cardiol. 2009; 16:351–7. [PubMed: 19247734]
6. Druz RS, Phillips LM, Chugkowski M, Boutis L, Rutkin B, Katz S. Wide-beam reconstruction half-time SPECT improves diagnostic certainty and preserves normalcy and accuracy: a quantitative perfusion analysis. J Nucl Cardiol. 2011; 18:52–61. [PubMed: 21181520]
7. DePuey EG, Bommireddipalli S, Clark J, Leykekhman A, Thompson LB, Friedman M. A comparison of the image quality of full-time myocardial perfusion SPECT vs wide beam reconstruction half-time and half-dose SPECT. J Nucl Cardiol. 2011; 18:273–80. [PubMed: 21287370]
8. Depuey EG, Ata P, Wray R, Friedman M. Very low-activity stress/high-activity rest, single-day myocardial perfusion SPECT with a conventional sodium iodide camera and wide beam reconstruction processing. J Nucl Cardiol. Jul 10.2012 [Epub ahead of print].
9. DePuey EG, Bommireddipalli S, Clark J, Thompson L, Srour Y. Wide beam reconstruction "quarter-time" gated myocardial perfusion SPECT functional imaging: a comparison to "full-time" ordered subset expectation maximum. J Nucl Cardiol. 2009; 16:736–52. [PubMed: 19533264]
10. Slomka P, Patton J, Berman D, Germano G. Advances in technical aspects of myocardial perfusion SPECT imaging. J Nucl Cardiol. 2009; 16:255–76. [PubMed: 19242769]
11. Garcia EV, Faber TL, Esteves FP. Cardiac dedicated ultrafast SPECT cameras: new designs and clinical implications. J Nucl Med. 2011; 52:210–7. [PubMed: 21233190]
12. Sharir T, Slomka P, Hayes S, et al. Multicenter trial of high-speed versus conventional single-photon emission computed tomography imaging: quantitative results of myocardial perfusion and left ventricular function. J Am Coll Cardiol. 2010; 55:1965–74. [PubMed: 20430269]
13. Sharir T, Ben-Haim S, Merzon K, Prochorov V, Dickman D, Berman D. High-speed myocardial perfusion imaging initial clinical comparison with conventional dual detector anger camera imaging. JACC Cardiovasc Imaging. 2008; 1:156–63. [PubMed: 19356422]
14. Herzog BA, Buechel RR, Katz R, et al. Nuclear myocardial perfusion imaging with a cadmium-zinc-telluride detector technique: optimized protocol for scan time reduction. J Nucl Med. 2010; 51:46–51. [PubMed: 20008999]
15. Buechel RR, Herzog BA, Husmann L, et al. Ultrafast nuclear myocardial perfusion imaging on a new gamma camera with semiconductor detector technique: first clinical validation. Eur J Nucl Med Mol Imaging. 2010; 37:773–8. [PubMed: 20107783]
16. Esteves FP, Raggi P, Folks RD, et al. Novel solid-state-detector dedicated cardiac camera for fast myocardial perfusion imaging: multicenter comparison with standard dual detector cameras. J Nucl Cardiol. 2009; 16:927–34. [PubMed: 19688410]
17. Bateman T, McGhie A, Courter S, Burgett E, Cullom J, Case J. Prospective study of ultra-low dose stress only solid-state SPECT: Comparison of efficiency, dosimetry and outcome versus traditional-dose attenuation-corrected stress-only anger SPECT (NCT01373944) [abstract]. J Am Coll Cardiol. 2012; 59:E1316.
18. Duvall WL, Wijetunga MN, Klein TM, et al. The prognosis of a normal stress-only Tc-99m myocardial perfusion imaging study. J Nucl Cardiol. 2010; 17:370–7. [PubMed: 20390394]
19. Chang SM, Nabi F, Xu J, Raza U, Mahmarian JJ. Normal stress-only versus standard stress/rest myocardial perfusion imaging: similar patient mortality with reduced radiation exposure. J Am Coll Cardiol. 2010; 55:221–30. [PubMed: 19913381]
20. Berman D, Abidov A, Kang X, et al. Prognostic validation of a 17-segment score derived from a 20-segment score for myocardial perfusion SPECT interpretation. J Nucl Cardiol. 2004; 11:414–23. [PubMed: 15295410]
21. Berman, D.; Germano, G. Interpretation and reporting of gated myocardial perfusion SPECT. In: Germano, G.; Berman, DS., editors. Clinical Gated Cardiac SPECT. 2. Oxford, U.K: Blackwell Publishing; 2006. p. 139-171.
22. Patton J, Slomka P, Germano G, Berman D. Recent technologic advances in nuclear cardiology. J Nucl Cardiol. 2007; 14:501–13. [PubMed: 17679058]
23. Gambhir S, Berman D, Ziffer J, et al. A novel high-sensitivity rapid-acquisition single-photon cardiac imaging camera. J Nucl Med. 2009; 50:635–43. [PubMed: 19339672]

24. Germano G, Kavanagh PB, Slomka PJ, Van Kriekinge SD, Pollard G, Berman DS. Quantitation in gated perfusion SPECT imaging: the Cedars-Sinai approach. J Nucl Cardiol. 2007; 14:433–54. [PubMed: 17679052]
25. Slomka P, Nishina H, Berman D, et al. Automated quantification of myocardial perfusion SPECT using simplified normal limits. J Nucl Cardiol. 2005; 12:66–77. [PubMed: 15682367]
26. Nakazato R, Tamarappoo BK, Kang X, et al. Quantitative upright-supine high-speed SPECT myocardial perfusion imaging for detection of coronary artery disease: correlation with invasive coronary angiography. J Nucl Med. 2010; 51:1724–31. [PubMed: 20956478]
27. Hachamovitch R, Hayes S, Friedman J, Cohen I, Berman D. Comparison of the short-term survival benefit associated with revascularization compared with medical therapy in patients with no prior coronary artery disease undergoing stress myocardial perfusion single photon emission computed tomography. Circulation. 2003; 107:2900–7. [PubMed: 12771008]
28. Germano G, Kiat H, Kavanagh PB, et al. Automatic quantification of ejection fraction from gated myocardial perfusion SPECT. J Nucl Med. 1995; 36:2138–47. [PubMed: 7472611]
29. Slomka P, Germano G, Kavanagh P, Javadi M, Berman D, Bengel F. Evaluation of a new automatic algorithm for quantification of ECG-gated 82Rb cardiac PET [abstract]. J Nucl Med. 2009; 50 (Suppl 2):1167.
30. Xu Y, Hayes S, Ali I, et al. Automatic and visual reproducibility of perfusion and function measures for myocardial perfusion SPECT. J Nucl Cardiol. 2010; 17:1050–7. [PubMed: 20963537]
31. Cerqueira MD, Allman KC, Ficaro EP, et al. Recommendations for reducing radiation exposure in myocardial perfusion imaging. J Nucl Cardiol. 2010; 17:709–18. [PubMed: 20503120]
32. Einstein AJ, Moser KW, Thompson RC, Cerqueira MD, Henzlova MJ. Radiation dose to patients from cardiac diagnostic imaging. Circulation. 2007; 116:1290–305. [PubMed: 17846343]
33. Berman D, Kang X, Gransar H, et al. Quantitative assessment of myocardial perfusion abnormality on SPECT myocardial perfusion imaging is more reproducible than expert visual analysis. J Nucl Cardiol. 2009; 16:45–53. [PubMed: 19152128]
34. Slomka P, Berman D, Germano G. Quantification of serial changes in myocardial perfusion. J Nucl Med. 2004; 45:1978–80. [PubMed: 15585470]

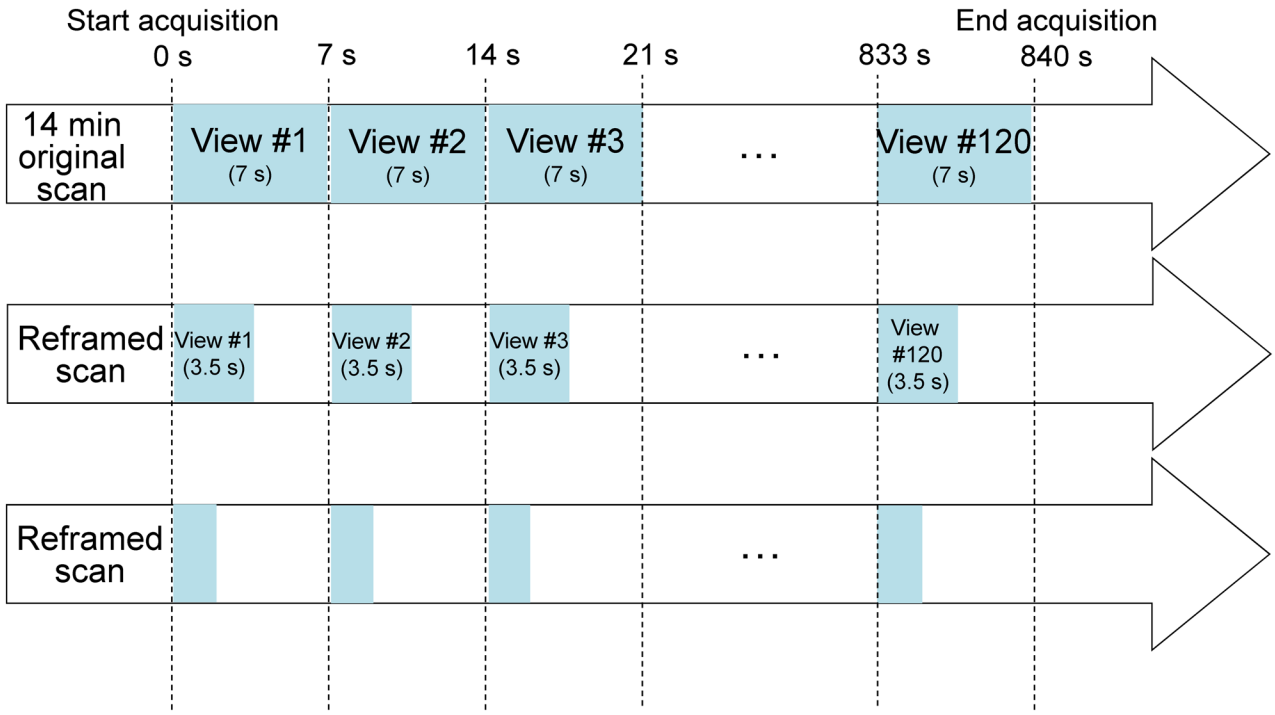

FIGURE 1.

Reframing Methodology. A time reframing for each view. Each CZT-SPECT clinical scan is done with 120 views generally between 1sec to 7sec per view. By selecting a part of each view we can reduce the scan time.

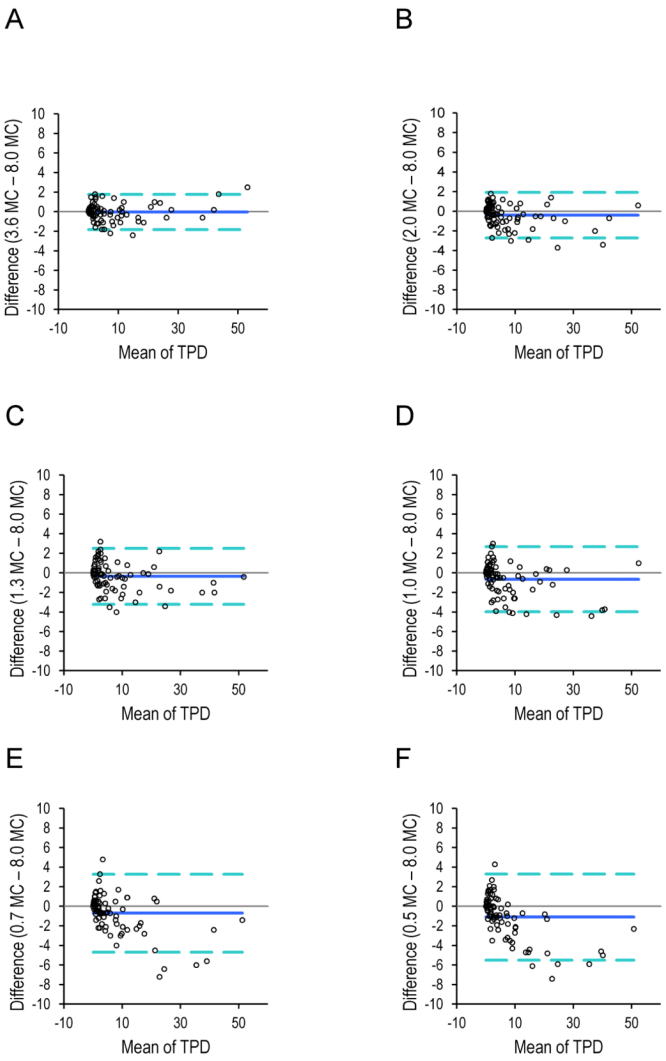

FIGURE 2.

Bland-Altman plots for TPD at different count levels (A: 3.6 MC, B: 2.0 MC, C: 1.3 MC, D: 1.0 MC, E: 0.7 MC, F: 0.5 MC) versus TPD for high-count scan (8.0 MC). Count-specific normal database was used for TPD.

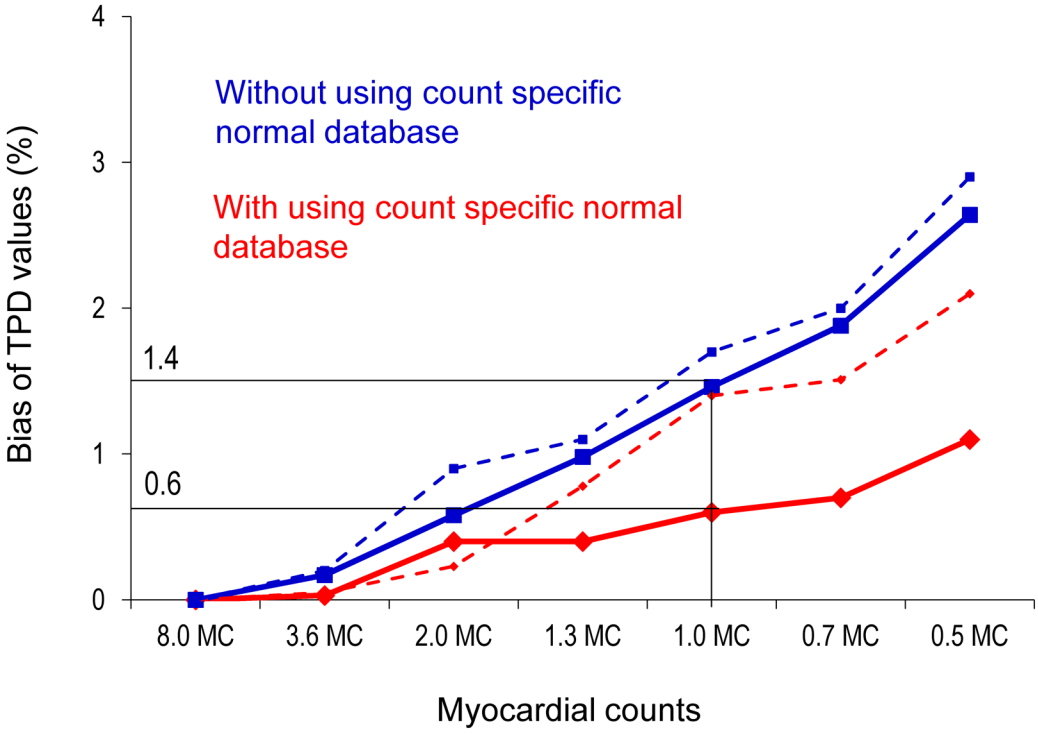

FIGURE 3.
TPD bias as a function of decreasing count levels with and without count-specific normal databases. Solid lines correspond to TPD bias for the overall population (n = 79). Dashed lines correspond to TPD bias for the abnormal stress perfusion patients (n = 32).

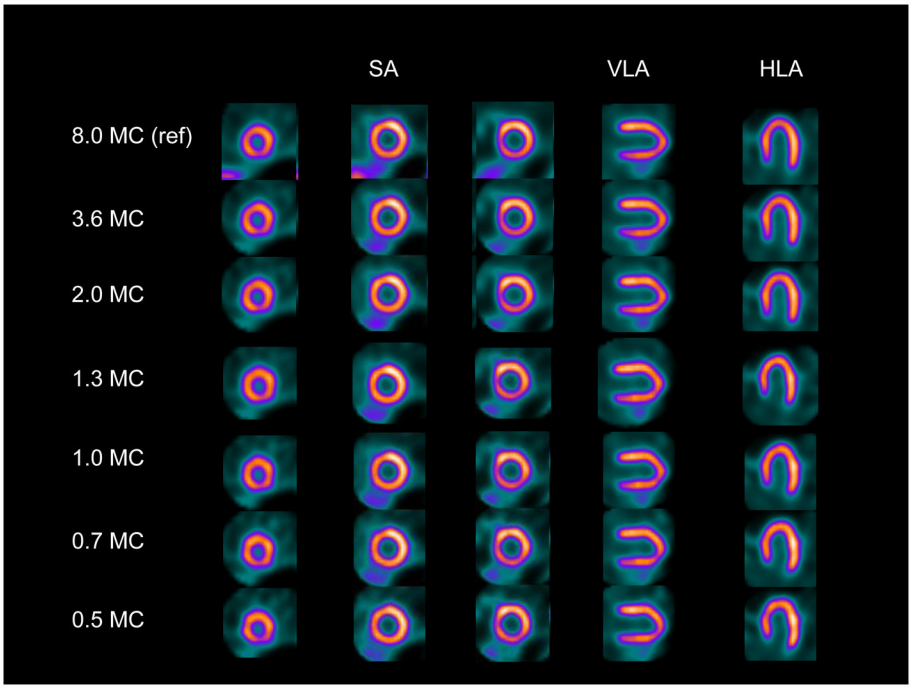

FIGURE 4.
Case example of normal perfusion images. SA = short axis; VLA = vertical long axis; HLA = horizontal long axis; MC = million counts. Original and all reframed scans had TPD of 0.

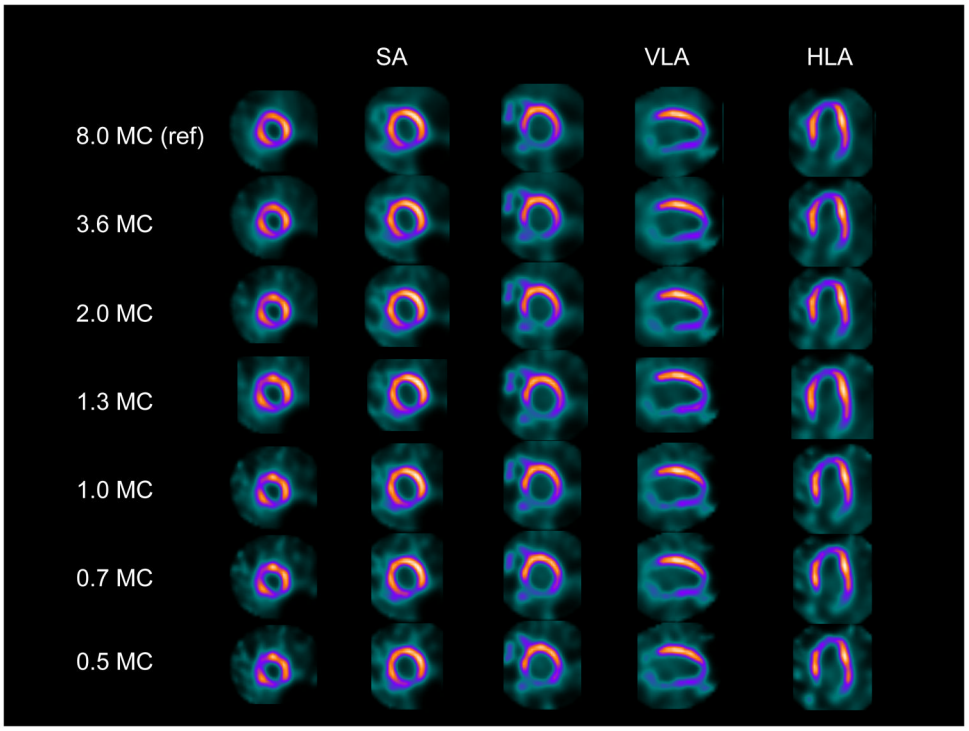

FIGURE 5.
Case example of abnormal perfusion images.TPD values were 11, 12, 12, 12, 12, 12, 9 for original, 3.6 MC, 2.0 MC, 1.3 MC, 1.0 MC, 0.7 MC and 0.5 MC, respectively.

TABLE 1

Patient Characteristics (n = 79)

Characteristic	Value
Male	38 (48%)
Age, years	65 ± 10
BMI, kg/m^2, (range)	30.0 ± 6.6 (20.2–54.0)
Hypertension	50 (63%)
Dyslipidemia	53 (67%)
Diabetes	19 (24%)
Current smoking	13 (16%)
Family history of CAD	30 (38%)
Previous myocardial infarction	14 (18%)
Previous PCI	12 (15%)
Previous CABG	15 (19%)
Exercise stress	40 (51%)

Data are mean ± SD, or number followed by percentage in parentheses.

BMI = body mass index; CAD = coronary artery disease; PCI = percutaneous coronary intervention; CABG = coronary artery bypass graft

TABLE 2

Number of Cases Required Contour Adjustment

Counts	Static QCed	Gate QCed
8.0 MC (ref)	1 (1%)	3 (4%)
3.6 MC	4 (5%)	4 (5%)
2.0 MC	2 (3%)	5 (6%)
1.3 MC	2 (3%)	6 (8%)
1.0 MC	1 (1%)	5 (6%)
0.7 MC	2 (3%)	4 (5%)
0.5 MC	2 (3%)	6 (8%)

MC, million counts

TABLE 3

Global Reproducibility of Perfusion and Function Parameters.

Counts	Correlation (TPD)	SD of differences (TPD)	Correlation (EF)	SD of differences (EF)
8.0 MC (ref)	ref	ref	ref	ref
3.6 MC	1.00	0.9	0.98	2.8
2.0 MC	0.99	1.1	0.98	3.1
1.3 MC	0.99	1.4	0.96	4.2
1.0 MC	0.99	1.7	0.97	4.2
0.7 MC	0.99	2.0	0.96	4.6
0.5 MC	0.99	2.2	0.96	4.7

Count-specific normal database was used for TPD. TPD = total perfusion deficit; SD = standard deviation, EF = ejection fraction

TABLE 4

Regional Reproducibility of Perfusion Parameters.

LAD		
Counts	**Correlation (TPD)**	**SD of differences (TPD)**
8.0 MC (ref)	ref	ref
3.6MC	1.00	0.6
2.0MC	1.00	0.6
1.3 MC	0.99	0.8
1.0 MC	0.99	0.8
0.7 MC	0.99	0.9
0.5 MC	0.99	1.1
LCX		
Counts	Correlation (TPD)	SD of differences (TPD)
8.0 MC (ref)	ref	ref
3.6 MC	0.99	0.5
2.0 MC	0.99	0.6
1.3 MC	0.96	1.1
1.0 MC	0.97	1.1
0.7 MC	0.96	1.1
0.5 MC	0.95	1.3
RCA		
Counts	Correlation (TPD)	SD of differences (TPD)
8.0 MC (ref)	ref	ref
3.6 MC	0.99	0.4
2.0 MC	0.99	0.4
1.3 MC	0.99	0.5
1.0 MC	0.99	0.5
0.7 MC	0.98	0.7
0.5 MC	0.96	1.0

Count-specific normal databases was used for TPD.